Requirements for the sampling source in coherent linear sampling

Inwoong Kim, Cheolhwan Kim, and Guifang Li

School of Optics/CREOL, University of Central Florida
4000 Central Florida Blvd., Orlando, FL 32816-2700
li@creol.ucf.edu

Abstract: Complex envelope measurement using coherent linear optical sampling with mode-locked sources is investigated. It is shown that reliable measurement of the phase requires that one of the optical modes of the mode-locked laser be locked to the optical carrier of the data signal to be measured. Carrier-envelope offset (CEO) is found to have negligible effect on the measurement. Measurement errors of the intensity profile and phase depend on the pulsewidth and chirp of the sampling pulses as well as the detuning between the carrier frequencies of the data signal and the center frequency of sampling source.

OCIS codes: (060.1660) Coherent communications, (120.5050) Phase measurement, (999.9999) Optical sampling.

References and links

1. M. H. Chou, I. Brener, G. Lenz, R. Scotti, E. E. Chaban, J. Shmulovich, D. Philen, S. Kosinski, K. R. Parameswaran, and M. M. Fejer, "Efficient wide-band and tunable midspan spectral inverter using cascaded nonlinearities in $LiNbO_3$ waveguides," IEEE Photon. Technol. Lett. **12**, 82–84 (2000).
2. S. Diez, R. Ludwig, C. Schmidt, U. Feiste, and H. G. Weber, "160-Gb/s optical sampling by gain-transparent four-wave mixing in a semiconductor optical amplifier," IEEE Photon. Technol. Lett. **11**, 1402–1404 (1999).
3. S. Kawanishi, T.Yamamoto, M. Nakawawa, and M. M. Fejer, "High sensitivity waveform measurement with optical sampling using quasi-phasematched mixing in $LiNbO_3$ waveguide," Electron. Lett. **37**, 842–844 (2001).
4. J. Li, J. Hansryd, P. O. Hedekvist, P. A. Andrekson, and S. N. Knudsen, "300 Gb/s eye-diagram measurement by optical sampling using fiber-based parametric amplification," IEEE Photon. Technol. Lett. **13**, 987–989 (2001).
5. S. Nogiwa, H. Ohta,Y. Kawaguchi, and Y. Endo, "Improvement of sensitivity in optical sampling system," Electron. Lett. **35**, 917–918 (1999).
6. J. Li, M. Westlund, H Sunnerud, B. Olsson, M. Karsson, and P. A. Adnrekson, "0.5-Tb/s eye-diagram measurement by optical sampling using XPM-induced wavelength shifting in highly nonlinear fiber," IEEE. Photon. Technol. Lett. **16**, 566-568 (2004).
7. C. Dorrer, C. R. Doerr, I. Kang, R. Ryfand, and P. J. Winzer, "High-sensitivity high-resolution sampling using linear optics and waveguide optical hybrid," OFC 2004, PDP18.
8. A. H. Gnauck, S. Chandrasekhar, J. Leuthold, and L. Stulz, "Demonstration of 42.7-Gb/s DPSK receiver with 45 photons/bit sensitivity," IEEE Photon. Technol. Lett. **15**, 99-101 (2003).
9. R. A. Griffin, R. L. Johnstone, R. G. Walker, J. Hall, S. D. Wadsworth, K. Berry, A. C. Carter, M. J. Wale, "10 Gb/s optical differential quadrature phase shift key (DQPSK) transmission using GaAs/AlGaAs integration," OFC 2002, FD6-1.
10. C. Dorrer, J. Leuthold, and C. R. Doerr, "Direct measurement of constellation diagrams of optical sources," OFC 2004, PDP33.
11. S. T. Cundiff, "Phase stabilization of ultrashort optical pulses," J. Phys. D: Appl. Phys. **35**. R43-R59 (2002).
12. A. Takada and W. Imajuku, "Linewidth narrowing and optical phase control of mode-locked semiconductor ring laser employing optical injection locking," IEEE Photon. Technol. Lett. **9**, 1328-1330 (1997).
13. R. F. Kalman, J. C. Fan, and L. G. Kazovsky, "Dynamic range of coherent analog fiber-optic links," J. Lightwave. Technol. **12**, 1263-1277 (1994).

#4157 - $15.00 US
Received 2 April 2004; revised 2 June 2004; accepted 3 June 2004

1. Introduction

Techniques for the measurement of high-speed temporal waveforms have advanced in response to demand in optical communication systems where per-channel data rate has approached 160 Gb/s and beyond. Traditional electronic measurement techniques using sample-and-hold circuits have given way to nonlinear optical sampling techniques [1]–[5]. In nonlinear optical sampling higher temporal resolution is achieved because a short optical pulse provides the gating function. Eye diagram measurement up to 500 Gb/s has been demonstrated [6]. This approach suffers from poor sensitivity because of the inherent low efficiency of nonlinear optical mixing. Recently, a new approach to optical waveform measurement based on coherent homodyne linear optical sampling has been demonstrated. Since ultra-short optical pulses are used in coherent linear optical sampling, it also provides high temporal resolution. Eye diagram measurement up to 640 Gb/s has been demonstrated [7]. Because coherent homodyne sampling is a linear process, measurement sensitivity ($3\cdot10^{3}\mathrm{mW}^{2}$) three orders of magnitude better than nonlinear optical techniques ($10^{6}\mathrm{mW}^{2}$) is possible [7]. Furthermore, coherent linear optical sampling offers the capability of measuring both the intensity and phase of optical signals, providing a timely diagnostic tool for investigating advanced modulation formats such as differential (quadrature) phase shift keying (DPSK/DQPSK) [8,9] before and after amplified fiber transmission where transmission impairments such as amplified spontaneous emission (ASE) can accumulated. In [10], the constellation diagram of DPSK signals at 10 and 40 Gb/s was measured experimentally. A deterministic rotation of the constellation diagram was observed and attributed to carrier-envelope offset (CEO) of the mode-locked laser. In this paper, we analyze the coherent linear sampling process and point out the actual mechanism for the rotation of the constellation diagram. In addition, we establish the requirements for the sampling pulses to eliminate this rotation and to achieve desired measurement accuracy for the phase and envelope profile.

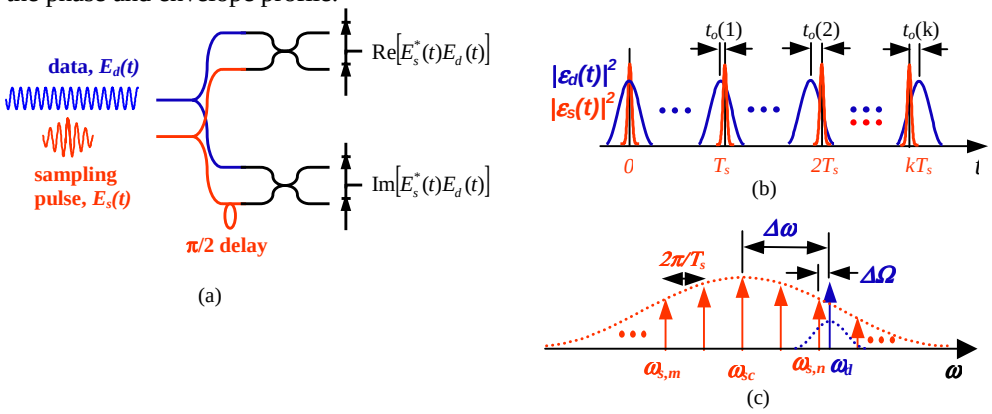

Fig. 1. (a) Schematic diagram of the linear optical sampling. Data and sampling pulses have the same polarization. (b) Walk off in the time domain between the sampling pulse (narrow) and data pulse (broad). (c) Schematic of the optical spectra of the data and sampling source: (ω_{sc} is the center frequency of the sampling source, ω_d is the optical carrier frequency of the data signal, $\Delta\Omega$, called carrier frequency offset, is the offset of the optical carrier of the data signal from the closest mode of the sampling source, and $\Delta\omega$, called carrier frequency detuning, is the detuning of the optical carrier of the data signal from the center frequency of the sampling source).

2. Analysis of linear optical sampling

The schematic diagram of linear optical sampling is shown in Fig. 1(a). The phase and intensity of the optical data signal, $E_d(t)$, are measured by observing its interference with two

#4157 - $15.00 US
Received 2 April 2004; revised 2 June 2004; accepted 3 June 2004

orthogonal quadratures of the sampling pulse, $E_s(t)$. In the upper branch, the balanced detectors measure the interference of the data signal and sampling pulse $\mathrm{Re}[E_s(t)^* E_d(t)]$. The sampling pulse is delayed in phase by $\pi/2$ before interfering with the data signal in the lower branch. The balanced detectors in the lower branch therefore measure the interference signal $\mathrm{Re}[\{E_s(t)e^{j\pi/2}\}^* E_d(t)] = \mathrm{Im}[E_s(t)^* E_d(t)]$. Therefore, the quadrature interference signals in the two branches together determine the complex quantity $E_s(t)^* E_d(t)$ completely (except a proportionality constant). High temporal resolution can be achieved even with low speed detectors by using a short sampling pulse, for example, from a mode-locked laser, which functions essentially as a gated local oscillator of coherent detection [7,10]. The interference between the data signal and sampling pulse occurs only during this gated duration.

The electric field of the mode-locked sampling pulse, $E_s(t)$, can be expressed as

$$E_s(t) = \sum_m a_m e^{j(\omega_{s,m}t+\phi_m)}, \quad \text{with } \omega_{s,m} = \frac{2\pi m}{T_s} + \alpha \tag{1}$$

where $\omega_{s,m}$ is the angular frequency of the mode, T_s is the period of the sampling pulse, a_m and ϕ_m are the amplitude and phase of the m_{th} mode. The parameter $0 < \alpha < 2\pi/T_s$ is a frequency offset that describes the CEO [11]. It is straightforward to verify that a nonzero offset leads to pulse-to-pulse relative shifts between the pulse envelope and the optical carrier. The sampling pulse train can also be decomposed into a slowly varying envelope around an optical carrier of center frequency $\omega_{sc} = 2\pi m_0/T_s$ as

$$E_s(t) = \left\{\sum_m a_m e^{j((\omega_{s,m}-\omega_{sc})t+\phi_m)}\right\} e^{j\omega_{sc}t} = \left\{\sum_m a_m e^{j(\frac{2\pi(m-m_0)}{T_s}t+\phi_m)}\right\} e^{j\omega_{sc}t} \tag{2}$$

As expected, the slowly-varying envelope (the summation in the brackets) is periodic with period T_s. The above expression can be rewritten by introducing a complex envelope function $\varepsilon_s(t)$ for a single pulse as

$$E_s(t) = \sum_l \varepsilon_s(t - l\,T_s)\, e^{j\omega_{sc}t} \tag{3}$$

For simplicity, let's assume that data pulse train is also periodic, for the time being, with a period T_d, given by

$$E_d(t) = \sum_l \varepsilon_d(t - l\,T_d)\, e^{j(\omega_d t+\phi_{do})} \tag{4}$$

where $\varepsilon_d(t)$ is the slowly-varying complex envelope profile for a single pulse, ω_d is the carrier frequency, ϕ_{do} is a constant initial phase, and T_d is the period of the data pulse.

When one is interested in measuring the constellation diagram of the data signals, the period of the sampling pulse is chosen to be exactly equal to the proper integer multiple of the period of the data signal. On the other hand, when one is interested in measuring the complex (intensity and phase) envelope of the data, it is convenient to make the period of the sampling pulses intentionally deviate slightly from an integer multiple of the period of the data signal so that successive sampling pulses sample the data pulses at different locations as shown in Fig. 1(b). When we assume that the peaks of the data pulse and the sampling pulse are aligned at $t = 0$ in Fig. 1(b), the off-set, $t_o(k)$, for the k_{th} sampling pulse is given by $t_o(k) = [(kT_s + 0.5T_d) \bmod T_d] - 0.5T_d$ where mod is the modulus function.

#4157 - $15.00 US
Received 2 April 2004; revised 2 June 2004; accepted 3 June 2004

With the above notations, the measured complex envelope by the k_{th} sampling pulse can be expressed as

$$\begin{aligned}\chi(k) &= \int_{(k-0.5)T_s}^{(k+0.5)T_s} E_s(t)^* E_d(t)\,dt \\ &= \int_{(k-0.5)T_s}^{(k+0.5)T_s} \varepsilon_s(t-kT_s)^* \varepsilon_d(t-kT_s+t_o(k)) e^{j((\omega_d-\omega_{sc})t+\phi_{do})}\,dt\end{aligned} \tag{5}$$

where the integration is due to the slow detector. Now let's assume that the carrier frequency of the data signal falls within the spectrum of mode-locked laser at an arbitrary position near one of the modes as shown on the Fig. 1(c) so that $\omega_d = \omega_{s,n} + \Delta\Omega$, where $\Delta\Omega$ is the carrier frequency offset. Then Eq. (5) becomes

$$\begin{aligned}\chi(k) &= \int_{(k-0.5)T_s}^{(k+0.5)T_s} \varepsilon_s(t-kT_s)^* \varepsilon_d(t-kT_s+t_o(k)) e^{j((\omega_{s,n}-\omega_{sc})t+\Delta\Omega t+\phi_{do})}\,dt \\ &= e^{j\phi_{do}} \int_{-0.5T_s}^{0.5T_s} \varepsilon_s(t')^* \varepsilon_d(t'+t_o(k)) e^{j\left[\frac{2\pi(n-m_0)}{T_s}t'\right]} e^{j\Delta\Omega(t'+kT_s)}\,dt' \\ &= e^{j\phi_{do}} e^{j\Delta\Omega kT_s} \int_{-0.5T_s}^{0.5T_s} \varepsilon_s(t')^* \varepsilon_d(t'+t_o(k)) e^{j\Delta\omega t'}\,dt'\end{aligned} \tag{6}$$

where we have used the fact that $\exp\left\{j\frac{2\pi(n-m_0)}{T_s}kT_s\right\} = 1$ and $\Delta\omega = \omega_d - \omega_{sc}$ is the carrier frequency detuning between the carrier frequencies. Let's assume that the sampling pulsewidth (Δt_s ,FWHM) is much smaller than the pulsewidth (Δt_d) of the data signal so that the envelope and phase of the data pulse are almost constant during sampling. Then Eq. (6) becomes

$$\begin{aligned}\chi(k) &\approx \varepsilon_d(t_o(k)) e^{j\phi_{do}} e^{j\Delta\Omega kT_s} \int_{-\infty}^{\infty} \varepsilon_s(t')^* e^{j\Delta\omega t'}\,dt' \quad (\text{for } \Delta t_s << \Delta t_d) \\ &= \varepsilon_d(t_o(k)) e^{j\phi_{do}} \tilde{\varepsilon}_s(\Delta\omega)^* e^{j\Delta\Omega kT_s}\end{aligned} \tag{7}$$

where $\tilde{\varepsilon}_s(\omega)$ is the Fourier transformation of the slowly varying envelope $\varepsilon_s(t)$. Equation (7) is the main results of the analysis of the linear optical sampling process. There are several important conclusions that can be derived from Eq. (7).

First, the CEO does not play any role in the measurement of the complex envelope of the data signal. This is because linear sampling is proportional to the interference between the optical carriers, integrated over the sampling pulse. This interference signal depends on the optical carrier frequency detuning only and is independent of CEO. This is clear as the parameter α is absent from Eq. (7). Second, when there is a carrier frequency offset, there will be a deterministic phase error for the measured signal. Consider the special case when the data pulses are uniform and the sampling pulse period is an integer multiple of the period of the data pulses. When the carrier frequency offset is zero, $\Delta\Omega = 0$, the measurement will yield an identical results for every sampling pulse as it should be as shown in Fig. 2(a). However, when $\Delta\Omega \neq 0$, the measurement will yield a different result for each sampling pulse which is rotated by phase angle of $\Delta\Omega T_S$ between successive sampling pulses, as shown in Fig. 2(b). It should be pointed out that the magnitude of the data signal will not be affected by this misalignment. The constellation diagram can be obtained without this deterministic rotation of phase by locking one of the modes of mode-locked laser to the optical carrier of the data signal. The periodic interference pattern between a mode-locked laser and a cw laser has been observed when one of the modes of the mode-locked laser is locked to the cw laser [12]. This rotation of the measured phase can potentially be corrected

#4157 - $15.00 US Received 2 April 2004; revised 2 June 2004; accepted 3 June 2004

using a proper software correction scheme [10], assuming that the frequencies of the data signal and the sampling source stay fixed during measurement. Third, the measured intensity ($\propto|\chi(k)|^2$) will be proportional to the spectral power density of the sampling pulse at the carrier frequency of the data signal as shown in Eq. (7). A quantitative example is given in Section 3 for the case of Gaussian pulses. This dependence of the measured intensity on the carrier frequency of the data signal should be taken into consideration when comparing measured results of different wavelength-division multiplexed (WDM) channels using the same sampling source.

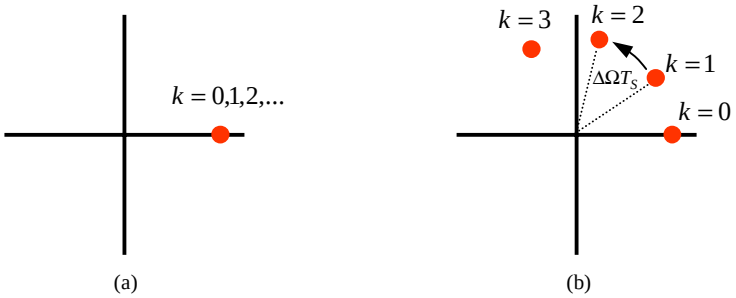

Fig. 2 Constellation diagram when the data phase is constant, (a) $\Delta\Omega = 0$ and (b) $\Delta\Omega \neq 0$.

3. Effects of chirp and finite pulsewidth of the sampling source

In this section, we describe the effects of the finite pulsewidth and linear chirp of the sampling pulses on the measurement of the complex envelope by retaining perturbation terms up to $(\Delta t_s / \Delta t_d)^2$, which were ignored in Eq. (7). As an example, we consider the case of Gaussian pulses for both sampling pulses and data pulses. The slowly varying envelope of the Gaussian sampling pulse is

$$\varepsilon_s(t) = \varepsilon_{s0} \frac{e^{-(1+iC)(2\ln 2\, t^2/\Delta t_s{}^2)}}{\sqrt{\frac{\sqrt{\pi}\,\Delta t_s}{2\sqrt{\ln 2}}}} \tag{8}$$

where C is the chirp parameter of the sampling pulse and the energy of a pulse is $|\varepsilon_{s0}|^2$. The data pulses are also Gaussian but with no chirp. Let's assume that one of the modes of the mode-locked laser is locked to the optical carrier of the data signal so that $\Delta\Omega = 0$ in Eq. (6).

It is straightforward to show that if the sampling pulsewidth is much smaller compared to the pulsewidth of the data signal, the measured pulsewidth is

$$\Delta t_d' \approx \Delta t_d \left[1 + \frac{1}{2(1+C^2)}\left(\frac{\Delta t_s}{\Delta t_d}\right)^2\right], \qquad (\Delta t_s{}^2 << \Delta t_d{}^2) \tag{9a}$$

$$= \Delta t_d \left[1 + \frac{8(\ln 2)^2}{\Delta t_d{}^2 \Delta\omega_s{}^2}\right], \qquad (\Delta t_s = \frac{4\ln 2\sqrt{1+C^2}}{\Delta\omega_s}) \tag{9b}$$

where $\Delta\omega_s$ is the spectral bandwidth (FWHM) of the sampling pulse. Eq. (9b) shows that the broadening of measured pulsewidth, $\Delta t_d' - \Delta t_d$, is inversely proportional to the square of the spectral bandwidth of sampling pulse and the pulsewidth of the data signal. For a fixed spectral bandwidth, chirp of the sampling source doesn't affect the measurement result. On the other hand, Eq. (9a) indicates that, for a fixed sampling pulsewidth, as chirp of the sampling pulse increases (bandwidth increases), the error in the measurement decreases. This is because the interference signals at the leading edge and trailing edge of the sampling pulse

#4157 - $15.00 US
Received 2 April 2004; revised 2 June 2004; accepted 3 June 2004

oscillate in time due to chirp. When integrated with a slow detector, the oscillating interference signals average to zero effectively narrowing the sampling pulsewidth.

As mentioned in the previous section, the intensity ($\propto |\chi(k)|^2$) of the complex envelope is proportional to the spectral power density of the sampling pulse at the carrier frequency of the data signal. For the Gaussian pulses considered here, the measured intensity is proportional to

$$\frac{|\varepsilon_{s0}|^2}{\Delta\omega_s} e^{-(4\ln 2)(\frac{\Delta\omega}{\Delta\omega_S})^2} \qquad (\Delta t_s{}^2 << \Delta t_d{}^2) \tag{10}$$

when a carrier frequency of the data signal is detuned from the center frequency of the Gaussian sampling pulse. A carrier frequency detuning of about $0.2\Delta\omega_s$ leads to a 10% reduction in measured intensity.

Assuming that the sampling pulsewidth is much smaller than that of the data signal, the measured phase error $\Phi(t_o(k))$ can be calculated from the phase of $\chi(k)$ in Eq. (6).

$$\begin{aligned} \Phi(t_o) &\approx \frac{2\ln 2\ C\Delta t_s{}^2 t_o{}^2 / \Delta t_d{}^2 - \Delta\omega\ t_o \Delta t_s{}^2}{(1+C^2)\Delta t_d{}^2}, \quad (\Delta t_s{}^2 << \Delta t_d{}^2,\ t_o < \Delta t_d/2) \\ &= \frac{32(\ln 2)^3 C t_o{}^2 / \Delta t_d{}^2 - 16(\ln 2)^2 \Delta\omega\ t_o}{\Delta\omega_s{}^2 \Delta t_d{}^2} \end{aligned} \tag{11}$$

The first term describes the quadratic phase measurement error due to chirp and the second term describes the linear phase measurement error due to carrier frequency detuning.

Numerical simulation was performed to confirm the analytic results presented above. The pulsewidth of the data signal was set to be 6.25 ps. The data pulse doesn't have any chirp and the phase was constant. The peaks of the envelope were normalized to unit value to compare the envelope profiles. The chirp of the sampling pulse and optical carrier frequency detuning were varied while the energy of the sampling pulse was fixed in the simulation. Two spectral bandwidths at 3.769 nm [Fig. 3(a)] and 1.767 nm [Fig. 3(b)] were used. For Fig. 3(a), the sampling pulsewidth was 0.9375 ps with no chirp, which is much smaller than the data pulsewidth and thus the analytical results of the previous section apply. The results of numerical simulation agree well with analytical results. For example, pulsewidth broadening was 69.9 fs and 70.3 fs , respectively, using numerical simulation and Eq. (9). The phase variations within the pulsewidth of the data signal were 0.011 radian with chirp only, 0.037 radian with detuning only, and 0.038 radian with both chirp and detuning.

#4157 - $15.00 US Received 2 April 2004; revised 2 June 2004; accepted 3 June 2004

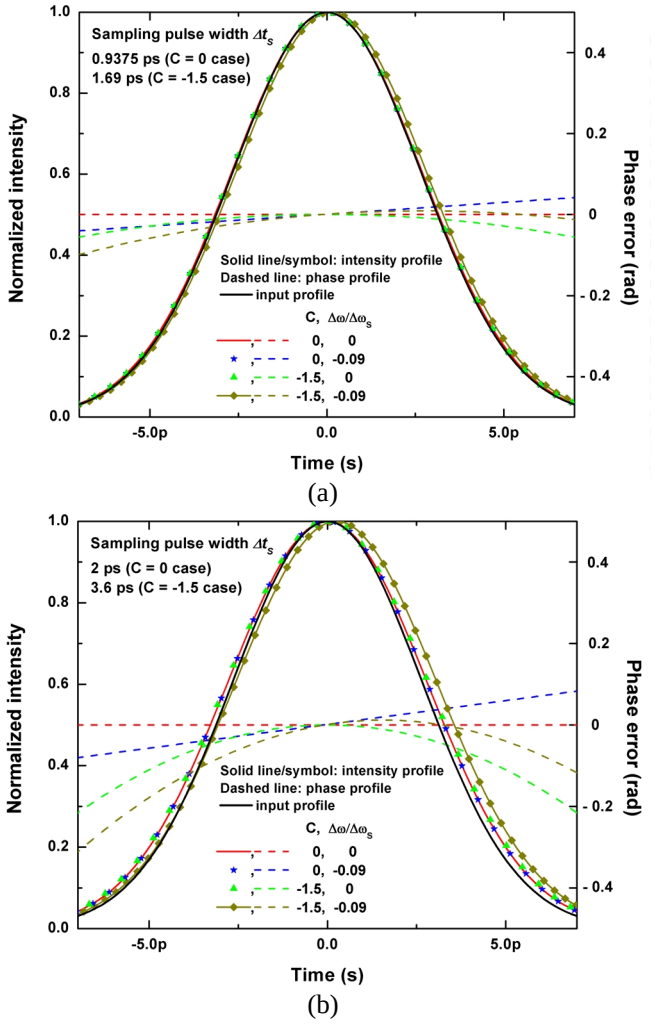

Fig. 3. Numerical simulation of measurement of the envelope profile and phase with linear optical sampling. The sampling pulse bandwidths are 3.769 nm (a) and 1.767 nm (b).

For Fig. 3(b), the sampling pulsewidth was 2 ps when there was no chirp and 3.6 ps when $C = -1.5$. The normalized carrier frequency detuning, $\Delta\omega/\Delta\omega_s$, was set to either zero or 0.09. Even though the sampling pulsewidth was large compared with that of the data pulse, the qualitative features predicted analytically remain valid. For the parameters chosen, the measured data pulse was broadened by only 5% even though the ratio of sampling pulsewidth to data pulsewidth is rather large. A temporal shift of the intensity profile was observed when there were both carrier frequency detuning and chirp in the sampling source. The phase variations within the pulsewidth of the data signal were 0.048 radian with chirp only, 0.074 radian with detuning only, and 0.095 radian with both chirp and detuning. Comparing the two chirp-only cases, it is verified that the phase error was reduced with increased sampling pulse bandwidth. In practice, linear chirp in the source can easily be compensated. The example here indicates that high-order chirp, which cannot be easily compensated, will result in phase measurement error. Simulation results for other pulse envelope profiles (such as raised cosine) agree qualitatively with the case for Gaussian pulses.

#4157 - $15.00 US
Received 2 April 2004; revised 2 June 2004; accepted 3 June 2004

4. Discussions and conclusions

In conclusion, we have analyzed the coherent linear optical sampling process. It is found that the measured intensity is proportional to the spectral power density of the sampling pulse at the carrier frequency of the data signal. Carrier frequency offset of the sampling source doesn't affect intensity measurement. Carrier frequency detuning results in a decrease in the measured intensity. Furthermore, in combination with chirp, carrier frequency detuning will lead to a temporal shift of the intensity profile. Reliable phase measurement requires that one of the modes of the sampling source be locked to the optical carrier of the data signal. Carrier frequency offset leads to a deterministic rotation of the phase angle between successive sampling periods for the constellation diagram measurement. Carrier frequency detuning (linear chirp) results in a linear (quadratic) phase error in the measurement of the complex envelope for Gaussian sampling pulses. Therefore it is very desirable to lock one of the modes of the mode-locked source to the carrier frequency of the data to remove carrier frequency offset. This has the added benefit of reducing the phase measurement error caused by random phase noise of the sampling source as briefly discussed below. Linear chirp should be compensated and high-order chirp should be minimized in the sampling source to reduce the phase measurement error. The sampling pulse width should be sufficiently small ($\Delta t_s / \Delta t_d < 0.2$) to ensure negligible broadening and temporal shift of the measured intensity profile.

In this paper we only investigated deterministic effects of the sampling source on linear optical sampling, which lead to measurement errors. The noise performance of the sampling source, on the other hand, will determine the intensity and phase measurement sensitivity. A complete analysis is beyond the scope of this paper. Here we will describe qualitatively the effect of noises in the sampling source. First, the intensity measurement sensitivity is determined by fluctuations of the energy of the sampling pulse. From the Eq. (7), the measured intensity, $\propto |\chi(k)|^2$, is proportional to envelope $|\varepsilon_d(t_o(k))|^2$ of the data pulse and also to the spectral power density $|\tilde{\varepsilon}_s(\Delta\omega)|^2$, which is proportional to the peak power of the sampling pulse. So the peak power fluctuations of the sampling pulses will directly affect the measurement of the intensity. However, the peak power of the sampling pulse can be monitored by a detector and this error may be reduced theoretically. Timing jitter of the sampling pulses will be added to the jitter of the data signal in a statistically independent manner. Second, the phase measurement sensitivity is determined by the statistical characteristics of the phase noise of the sampling source and measurement duration. For the special case where each mode of the mode-locked laser has the same phase noise (linewidth) because of coherence, the sampling pulse can be expressed as

$$E_s(t) = \sum_l \varepsilon_s(t - lT_s) e^{j[\omega_{sc}t + \phi_N(t)]} \tag{12}$$

where $\phi_N(t)$ is a random process. An additional phase $\phi_N(kT_s)$ will be added to the measured phase of the data signal. The sensitivity of phase measurement will be given by $<\phi_N^2>$, which is related to the linewidth of modes as $<\phi_N{}^2> = \Delta\nu(1/f_2 - 1/f_1)/\pi$ where $\Delta\nu$ is the linewidth of each optical mode of the sampling source and f_1 (f_2) is the upper (lower) frequency limit of the measurement [13]. The upper limit is determined by the sampling pulsewidth. The lower limit is the inverse of the observation period.

#4157 - $15.00 US Received 2 April 2004; revised 2 June 2004; accepted 3 June 2004